Surgical and Radiologic Anatomy (2019) 41:209–219
https://doi.org/10.1007/s00276-018-2145-7

ORIGINAL ARTICLE

Analysis of the development of human foetal nasal turbinates using CBCT imaging

Rieko Asaumi[1] · Yoko Miwa[2] · Taisuke Kawai[1] · Iwao Sato[2]

Received: 21 August 2018 / Accepted: 26 November 2018 / Published online: 6 December 2018
© Springer-Verlag France SAS, part of Springer Nature 2018

Abstract

Purpose The morphological structure of the nasal cavity (NC) is important for endoscopic surgical treatment. The location of nasal turbinates, including the superior turbinate (ST), middle turbinate (MT) and inferior turbinate (IT), are well presented during the formation of the human NC in cone beam CT (CBCT) images. There is a complex relationship between the nasal sinuses, the maxillary sinus (MS), ethmoidal sinus and sphenoid sinus, during formation of the NC structure at the morphological level. There is a need to clearly define the relationships of these nasal elements at the ossification level, during development.

Methods We investigated the three-dimensional construction of human foetal NC elements, including ST, MT, IT and vomer, using CBCT images from 16 weeks gestation (E16) to E31 (25 foetuses) and compared it to histochemical observations (E25).

Results At the stage of ossification, the studied elements are elongated in the posterior region near the sphenoidal bone, showing that the locations of the ST, MT, and IT are important during formation of the NC. CBCT analysis revealed that the horizontal and vertical directions of nasal turbinates affect the formation of the human NC.

Conclusion The location and elongated development of the MT is one of the most important elements for NC formation. The relationship between the nasal sinus and nasal turbine at the level of ossification may provide useful information in clinical treatment of children.

Keywords CBCT · Nasal turbinate · Nasal cavity · Maxillary sinus · Foetus

Introduction

The lateral nasal wall is an important anatomical landmark for endoscopic surgical treatment. Understanding the anatomy of the nasal sinuses and nasal turbinates forms the basis of safe and effective endoscopic surgery. Preoperative identification and intraoperative localization of the anatomical features of the nasal wall are key to successful clinical treatment. Many reports have indicated that the nasal sinuses, including the maxillary sinus (MS), ethmoidal sinus and sphenoid sinus, have some effect on the nasal cavity (NC) structure [2, 6, 11, 14, 21]. The formation of nasal turbinate results from the combined action of bipedalism, eye positioning, regression of the midface, and cerebral lobe enlargement [17, 20]. Recently, Jankowski et al. [7] reported that the evo–devo theory offers a rational explanation to describe the complex formation of the turbinate of the ethmoid bone. During development, the vomer (V) and inferior turbinate bones are also derived from the secondary palate of the maxillary process. However, there is a little information regarding the formation of the NC and nasal turbinate at the levels of ossification.

Knowledge of the possible diseases of the paediatric nose and the nasal sinuses, as well as the neighbouring anatomical structures, is important for treatment [24]. During the 7th week, the first buds of the three turbinates begin to appear; the pre-cartilaginous nucleus of the inferior turbinate (IT) is observed during the 9th week of the development of the nose area. Then, the uncinate process begins to appear and the invagination of the epithelium initiates the formation of the infundibulum and the MS at the 10th week. The IT

✉ Iwao Sato
iwaoa1@tokyo.ndu.ac.jp

[1] Department of Oral and Maxillofacial Radiology, School of Life Dentistry at Tokyo, The Nippon Dental University, 1-9-20 Fujimi, Chiyoda-ku, Tokyo 102-8159, Japan

[2] Department of Anatomy, School of Life Dentistry at Tokyo, The Nippon Dental University, 1-9-20 Fujimi, Chiyoda-ku, Tokyo 102-8159, Japan

develops by endochondral ossification of components of the mesethmoid and ethmoid. The chondral framework of the IT undergoes ossification during the 5th and 7th month of foetal life [1, 3, 5]. Hypertrophy of the IT and concha bullosa are causes of nasal obstruction. Neskey et al. [19] showed that anatomic variations, such as deviated nasal septum, IT hypertrophy, paradoxical middle turbinate (MT) and concha bullosa, were all associated with surgical removal of nasal obstructions. The developing nasal turbinate ossifications are rarely seen from E24 weeks to E31. Cone beam CT (CBCT) is a widely used imaging modality on dentistry and otorhinolaryngology due to its ability to acquire high-resolution images of the hard tissues in a non-invasive manner. Therefore, the aim of this study was to investigate the formation of nasal turbinates at the ossification stage from 16 to 31 weeks using the CBCT analysis.

Materials and methods

Subjects

We examined 25 human foetuses from E16 to E31 for this study (18 males and 7 females). The foetuses were obtained with full consent given by the family from induced abortions and spontaneous abortions. Ethical consent was also achieved from the Donation for Human Dissection and collection at Nippon Dental University. The approximate age of each foetus was determined according to Streeter's tables [25].

CBCT scanning

The CBCT used was a PSR 9000N (Asahi Roentgen Industry, Kyoto, Japan). Images around the NC of specimens were acquired from samples of E16–E31. The CBCT scans were operated at tube potential 60 kV, tube current 4 mA, the scan time of 20 s, and acquired cylindrical areas of Ø41 × 40 mm with high resolution (voxel size: 0.1 mm).

A three-dimensional structure of the NC of human foetuses with CBCT images was reconstructed using the software Materialize Mimics Innovation Suite for Research (Materialize, Leuven, Belgium). The structure of the nasal turbinate was measured using the software Image J ver. 1.51 (NIH, Maryland, USA). The CBCT images were observed in the palatal plane (PP) in a horizontal reference plane and the median sagittal plane in a vertical reference plane.

Measurement points and identification of each turbinate

We defined measuring points of CBCT images as follows (see Fig. 1a–g); D1, horizontal distance between ANS (anterior nasal spine) and PNS (posterior nasal spine); D2, anterior–posterior length of the V; D3, anterior–posterior length of the IT; D4, anterior–posterior length of the MT; D5, anterior–posterior length of the superior turbinate (ST). H0, vertical length from the PP to the bottom of the nasal bone (NB); H1, vertical height between the top and bottom of the V; H2, vertical height of the IT; H3, vertical height of the MT; H4, vertical height of the ST. W1, mesio–distal distance between the M (midline) and the most mesial position of the IT; W2, mesio–distal distance between the M and the most mesial position of the MT; W3, mesio–distal distance between the M and most mesial position of the ST; PH1, vertical height between the lowest position of the IT and the PP; PH2, vertical height between the lowest position of the MT and the PP; and PH3, the vertical height between the lowest position of the ST and the PP. We also defined the structures of the turbinates using CBCT images with high resolution (voxel size: 0.1 mm). From each section, several points were selected from the border of IT and MT. These points were reconstructed to a 3D image using a commercial software (Materialize Mimics Innovation Suite for Research, Materialize, Leuven, Belgium).

Histological analysis

The specimens were selected from the Department of Dentistry, Nippon Dental University Collections. Three male human foetuses were used for histochemical observation at E25. The specimens were embedded in paraffin, cut frontally, horizontally and sagittally to obtain serial sections of 6 µm thickness. These sections were deparaffinized with xylene, dehydrated using a series of ethanol and then stained using haematoxylin and eosin, for light microscopic examination.

Statistical methods

The differences in bone structure and density amongst the samples used were assessed using Student's *t* test and two-way analysis of variance (ANOVA), followed by Tukey's post hoc test. Differences were considered significant when $p < 0.05$. The statistical analyses were performed using IBM SPSS statistics software (Base, version 22) (New York, USA).The results were reported as mean ± SD.

Ethics

The human foetuses were collected at Nippon Dental University and were obtained complying with the Law Concerning Cadaver Dissection and Preservation.

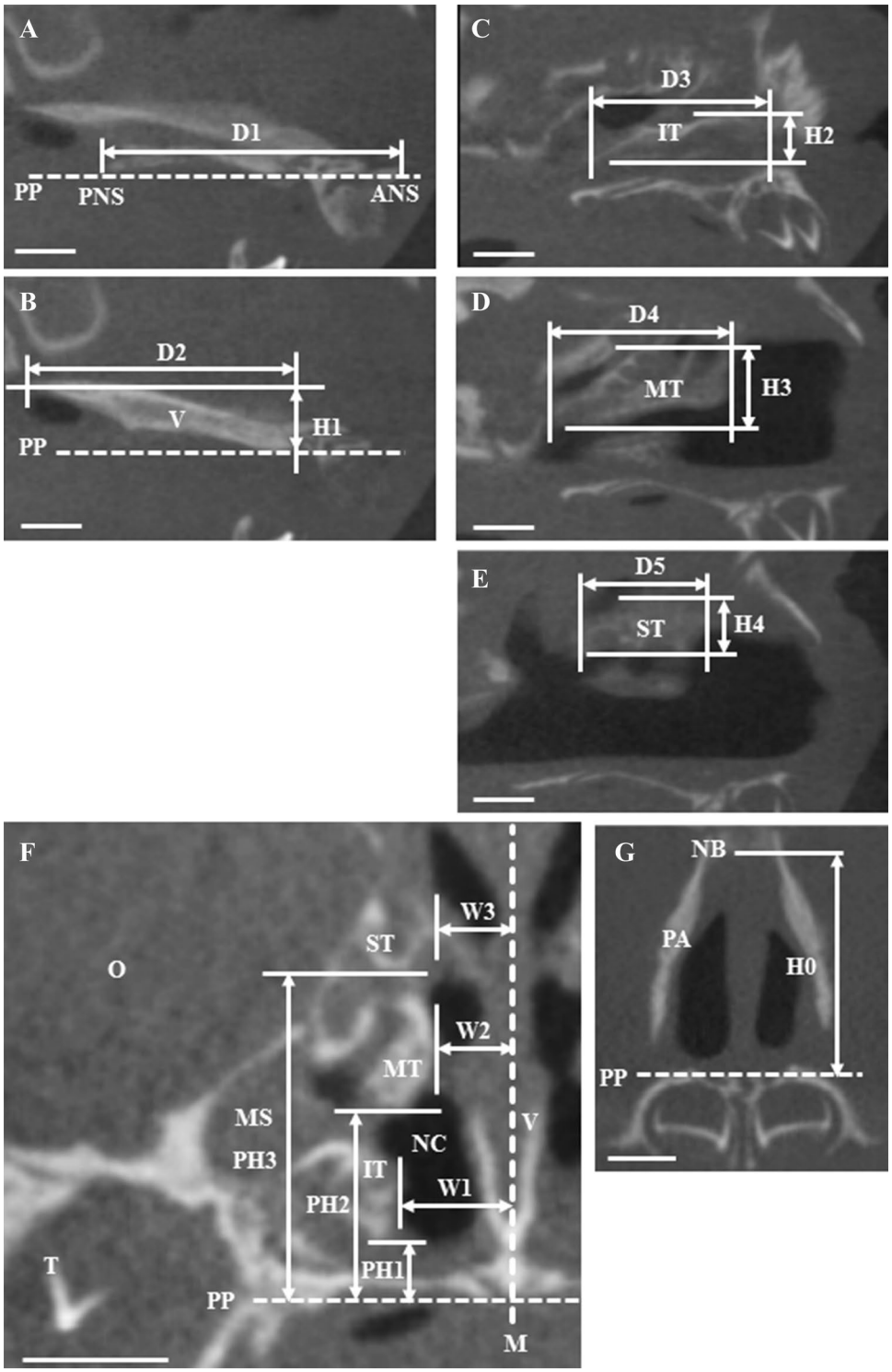

Fig. 1 Measurement points of CBCT images. **a** a sagittal CBCT image on the M. D1, horizontal distance between ANS and PNS. **b** a sagittal CBCT image on the V. H1, vertical height between top and bottom of the V; D2, anterior–posterior length of the V. **c** a sagittal image of the MT. D3, anterior–posterior length of the IT; H2, vertical height of the IT. **d** a sagittal image of the IT; D4, anterior–posterior length of the MT; H3, vertical height of the MT. **e** a sagittal image of the ST. D5, anterior–posterior length of the ST; H4, vertical height of ST. **f** a coronal CBCT image around the NC. W1, mesio–distal distance between M and most mesial position of the IT; W2, mesio–distal distance between M and the most mesial position of the MT; W3, mesio–distal distance between M and most mesial position of the ST; PH1, vertical height between the lowest position of the IT and the PP; PH2, vertical height between the lowest position of the MT and the PP; PH3, vertical height between the lowest position of the ST and the PP. **g** a coronal CBCT image around the maxillary deciduous central incisors. H0, vertical length of from the PP to the bottom of the NB. *ANS* anterior nasal spine, *PNS* posterior nasal spine, *IT* inferior turbinate, *M* midline, *MS* maxillary sinus, *MT* middle turbinate, *NB* nasal bone, *NC* nasal cavity, *O* orbit, *PA* piriform aperture, *PP* palatal plane, *ST* superior turbinate, *T* tooth, *V* vomer, bar = 5 mm. (Color figure online)

Results

CBCT 3D images from E17 to E31 (see Figs. 2, 3, 4, 5)

In the sagittal CBCT image of the E17 head, the Y-like structure of V was recognized as a structure with a thin elongated rhombus, and the anterior region of the V was located at the maxilla adjacent to the NC side of the maxilla. The V was elongated to the palatine bone and reached the posterior regions of the body of the sphenoid bone. The anterior portion of the V was located on the NC side of the maxilla that was also at the posterior side of the second deciduous

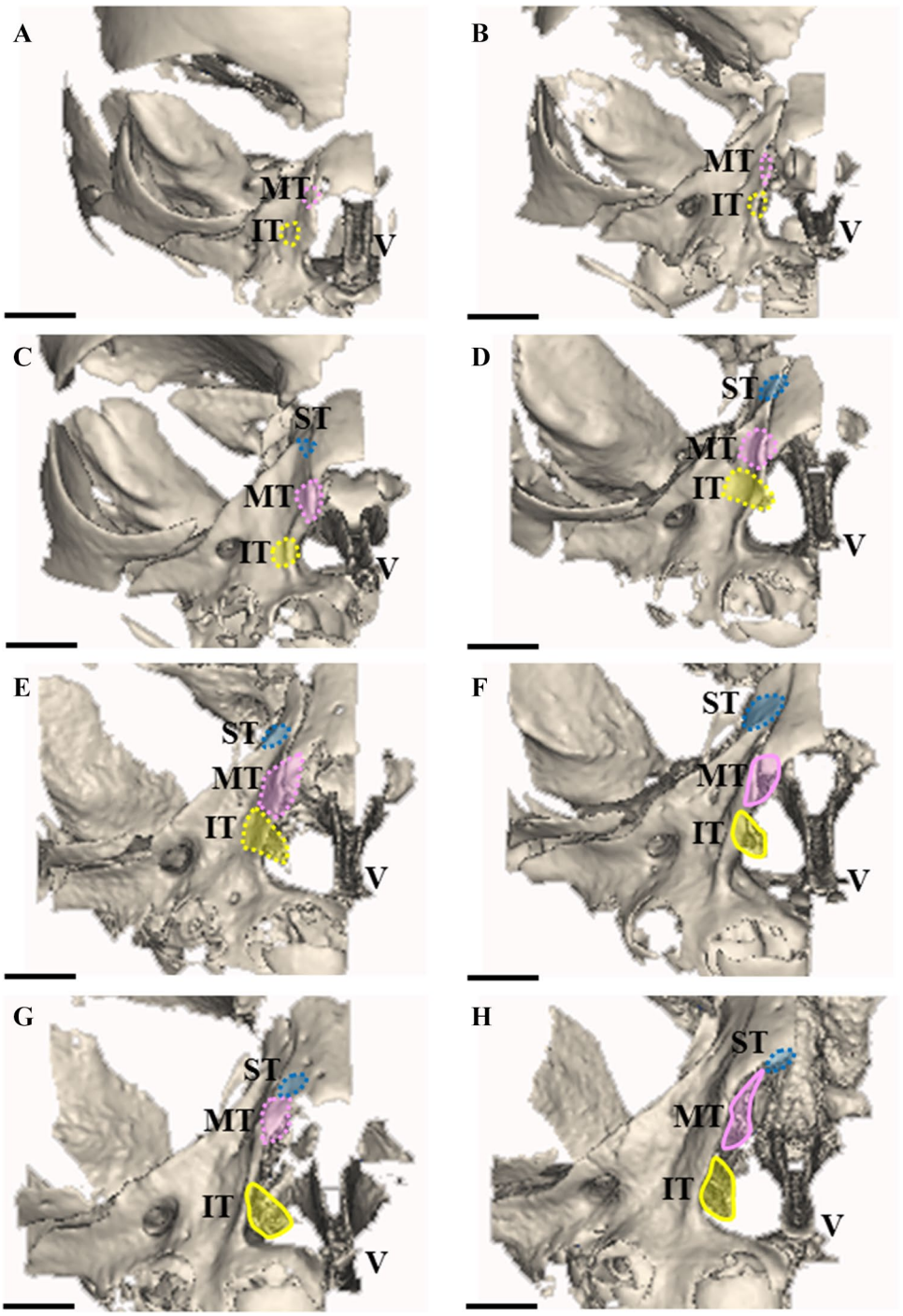

Fig. 2 The 3D frontal view images of NC with V, MT, IT, ST in human foetuses from 17 weeks gestation to 31 weeks gestation (**a** E17; **b** E19; **c** E21; **d** E23; **e** E25; **f** E27; **g** E29; **h** E31). *IT* inferior turbinate, *MT* middle turbinate, *ST* superior turbinate, *V* vomer, bar = 5 mm. (Color figure online)

incisor. The IT appeared as a thin rod-like structure composed of a few small masses of low density. They lined up in the anterior and posterior directions, and the V was present at a portion behind the IT. In the frontal part of the CBCT image, the MT was a small structure with very low density, located at the upper portion of the IT. The crista galli, the cribriform plate, the ST and the ethmoidal labyrinth were not fully calcified. In the sagittal image of the E19 head, the V was almost at the same position as at E17, however, the anterior side of the V is located at the position between the first deciduous incisor teeth and the second deciduous incisor teeth of the maxilla. Even during this period, the crista galli, the cribriform plate, the ST and the ethmoidal labyrinth were also not fully calcified. In the sagittal image of E21, the V was almost at same the position and structure as in the E19 head; however, the MT was recognized as a somewhat developed rhomboid-shaped calcified structure. The anterior side of the V is located at a position between the

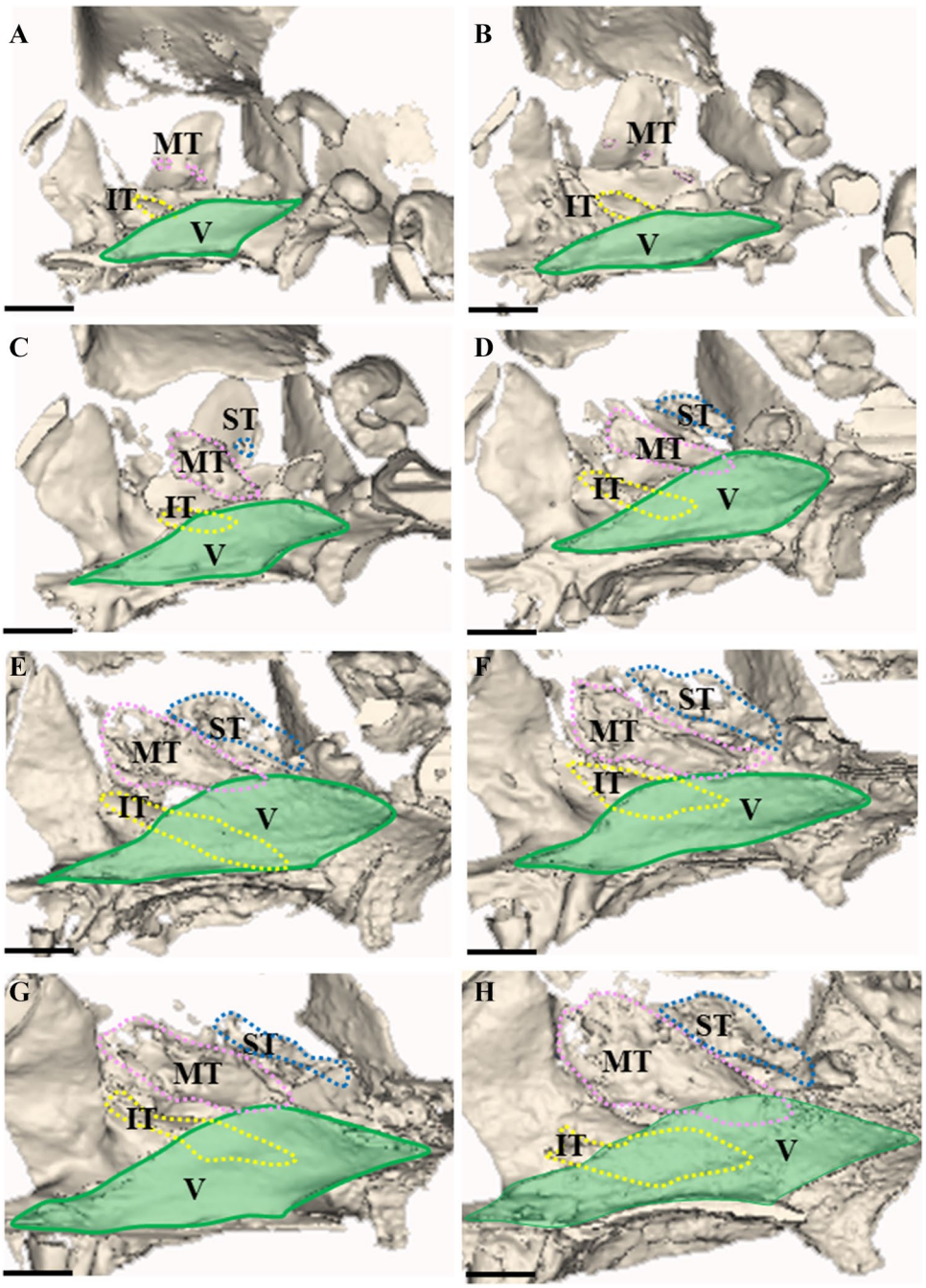

Fig. 3 The 3D sagittal view images of the NC with V, MT, IT, ST in human foetuses from 17 weeks gestation to 31 weeks gestation (**a** E17; **b** E19; **c** E21; **d** E23; **e** E25; **f** E27; **g** E29; **h** E31). *IT* inferior turbinate, *MT* middle turbinate, *ST* superior turbinate, *V* vomer, bar = 5 mm. (Color figure online)

first deciduous incisor teeth and the second deciduous incisor teeth of the maxilla, and the posterior side was located at the anterior region of the body of the sphenoid bone. In the frontal head CBCT image, the MT was located at the superior part of the V. The crista galli, the cribriform plate, the ST and the ethmoidal labyrinth were not yet calcified. In the sagittal image of the E23 head, the V was recognized as a developed elongated and widely rhomboid structure, ranging from the anterior side of the second deciduous incisor teeth of the maxillary bone to the palatine bone and the body of the sphenoid bone. The MT developed calcification somewhat, recognized as an elongated structure, and the anterior portion beginning from the position of the posterior part of the nasolacrimal duct and the posterior part reached near the palatine bone of the horizontal plate. In the sagittal image, the middle part of the IT was located behind the V. The ST was recognized as a calcified stick structure. The ST was located from the adjacent part of the nasal bone in the anterior direction and reached near the palatal projection of the maxilla and the palatal bone horizontal plate boundary. In the frontal image, it was located in the order of the IT, the MT and the ST. The crista galli, the cribriform plate, the

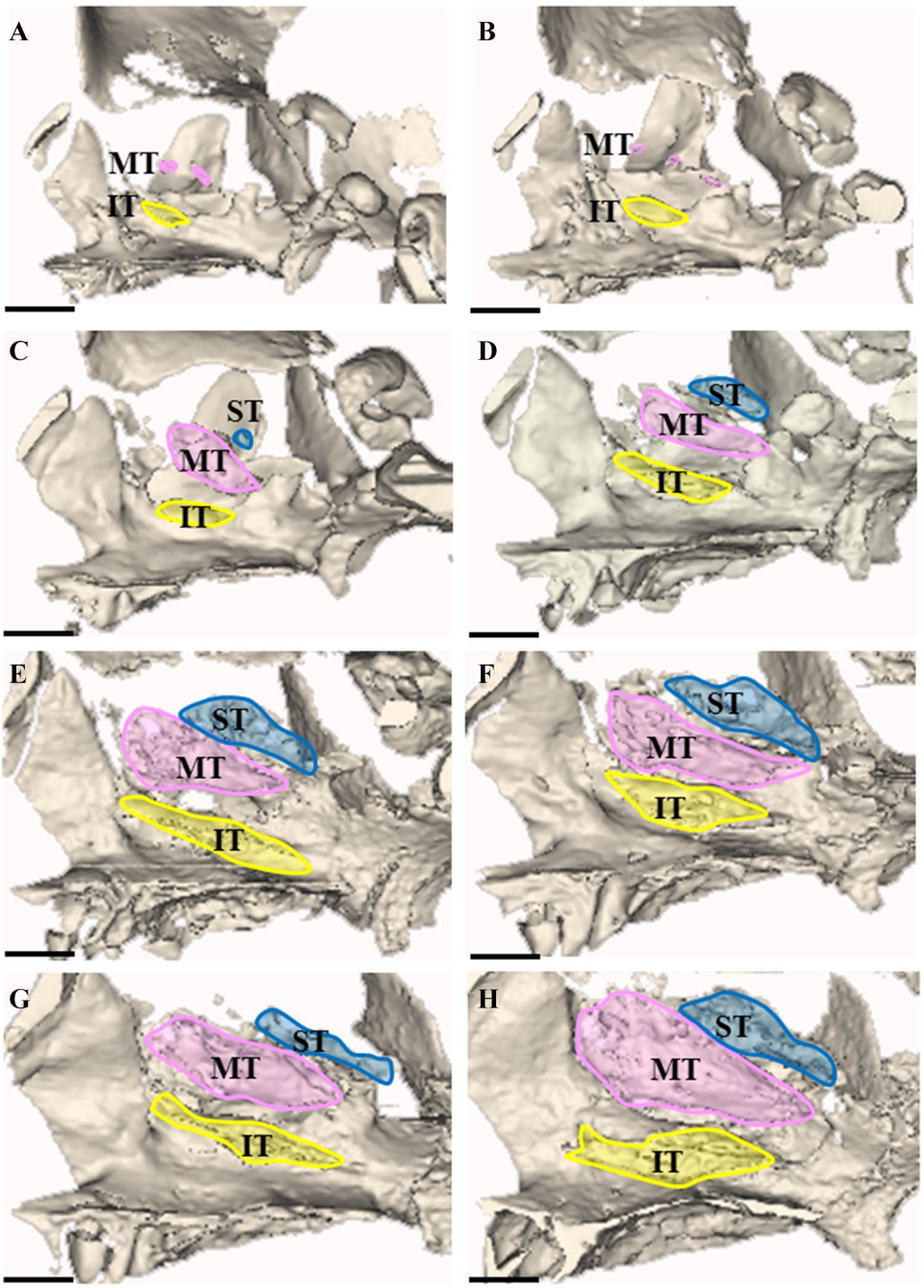

Fig. 4 The 3D sagittal view images of the NC with MT, IT, ST except for the V in human foetuses from 17 weeks gestation to 31 weeks gestation (**a** E17; **b** E19; **c** E21; **d** E23; **e** E25; **f** E27; **g** E29; **h** E31). *IT* inferior turbinate, *MT* middle turbinate, *ST* superior turbinate, *V* vomer, bar = 5 mm. (Color figure online)

ST and the ethmoidal labyrinth were also not yet calcified. In the sagittal image of the E25 head, the V was recognized as a developed rhomboid-shaped structure having a wide central portion. It was located at the maxilla, palatine bone and the sphenoid bone, and the beginning portion of V was at the first deciduous teeth. It was adjacent to the body of the sphenoid bone. The IT appeared as an elongated structure with a wide anterior portion. Nearly two-thirds of the IT was present at the position of the shadow of the V, and the IT was recognized as a rhomboid-shaped structure having a slightly wide portion. The beginnings of the IT and the MT were from the posterior part of the nasolacrimal duct. The posterior border of the IT was close, between the horizontal plate of the palatal bone and the sphenoid bone. The MT was near the boundary between the palatine bone and the maxilla. In the sagittal E25 image, the ST was recognized as a somewhat wide rhomboid-shaped structure in the anterior direction. The ST started from the adjacent part of the nasal bone in the anterior direction and reached near the central part of the palatal bone horizontal plate. In the frontal E25 image, the ST contributed a part of orbit, and IT was seen in a form hanging down from the piriform aperture. In the

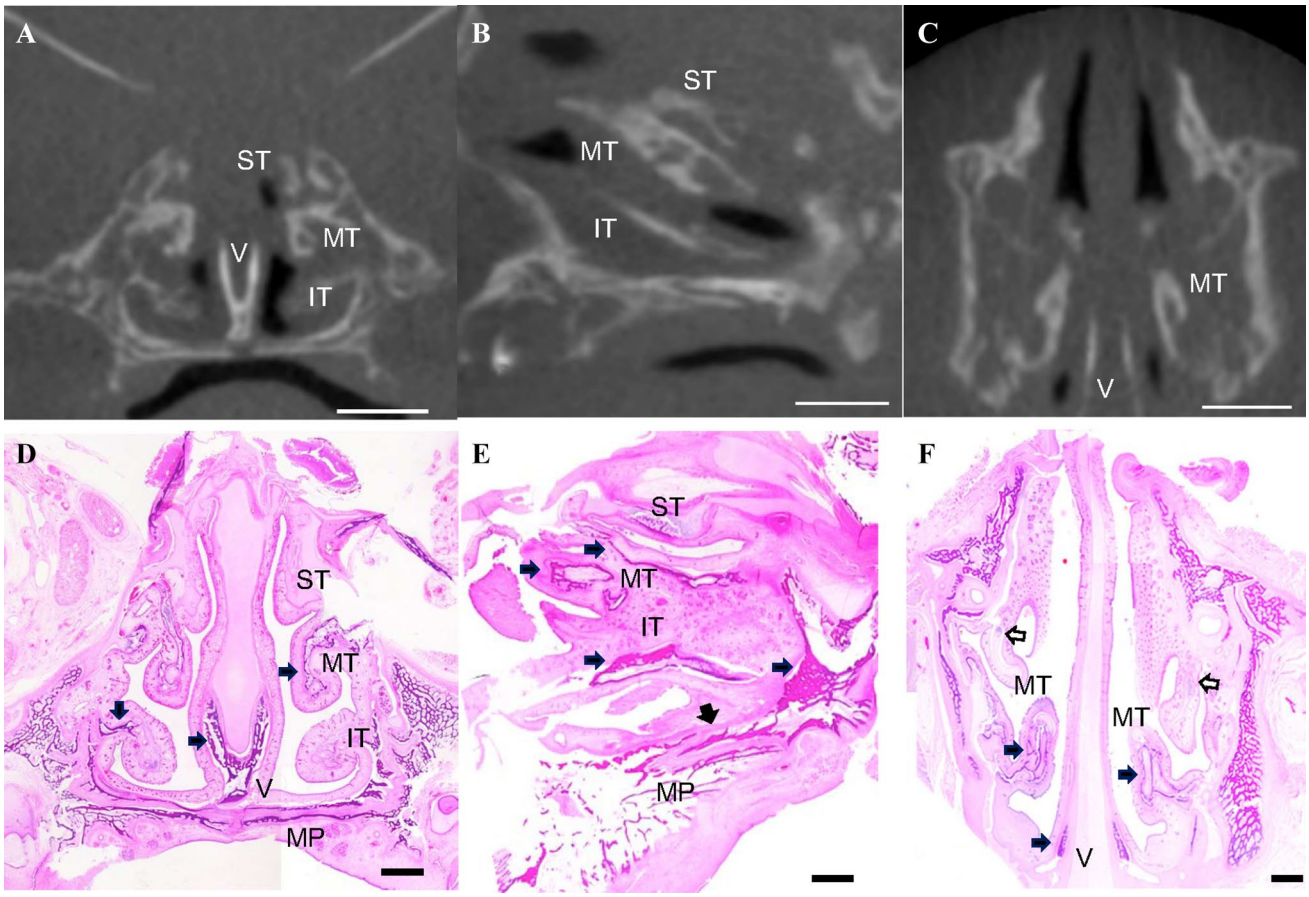

Fig. 5 The frontal, horizontal, and sagittal HE sections at E25. The developed nasal turbinates, including ST, MT and IT were appeared in the nasal cavity with the lateral masses of the ethmoid at frontal section. The woven bone structures (black arrows) were found in the maxilla, V and ethmoid bone. The weak ossify zone (white arrows) appeared at the end of the anterior region of MT and IT. In the sagittal section, the thin and elongated ossify structures of the MT and IT (black arrows) were recognized like that of the calcified stick-like structure of CBCT image of E25. **a** Frontal section with CBCT image; **b** sagittal section with CBCT image; **c** horizontal section with CBCT image; **d** frontal section with hematoxylin and eosin (HE) staining; **e** sagittal section with HE staining; **f** horizontal section with HE staining. **a**–**c** Bar = 5 mm, **d**–**f** bar = 1 mm. (Color figure online)

sagittal image of E27 and E29 heads, CBCT images showed almost the same morphology as at E25. The ST was recognized as a slightly widely rhomboid structure in the anterior direction, starting from the adjacent part of the nasal bone and the posterior side reaching near the adjacent part of the palatal bone, horizontal plate and sphenoid bone. At E31, approximately two-thirds of the IT was located at the shadow of the V. The IT was the boundary between the maxillary bones. For the palatine bones, the MT was the boundary between the palatine bone horizontal plate and the sphenoid bone. By contrast, the ST began from the middle part of the maxilla, and the ST extended to the base of the greater wing of the sphenoid bone. In the frontal CBCT images, the IT and the MT were slightly separated, and the MT and the ST showed adjacent images. The V was recognized as a large structure with a large rhombus developed from the anterior nasal spine of the maxilla to the body of the sphenoid bone with a widely developed central part region.

Properties of CBCT measurements of the nasal turbinates

We measured correlations between nasal turbinates and the age of 16 reference points as follows: horizontal distance (D1–5), vertical length (H0–H4), mesio–distal distance (W1–W3) and vertical height (PH1–3) (see Table 1). However, there were no differences between left and right and gender for these measurement data. We also classified three groups of gestations, including E16–E20, E21–E25 and E26–E31, for a measurement analysis of nasal turbinates. Significant differences were found in the D1–D5 of E21–E25 and E26–E31 (almost $p < 0.001$). The same significant differences were also found in the H0–H4 of E26–E31 ($p < 0.001$). Significant differences were found in the H2, 3, 4 of E21–E25 ($p < 0.001$). Significant differences were found in the H0 of E21–E25 ($p < 0.01$) and H1 of E21–E25 ($p < 0.05$). However, significant differences

Table 1 The correlation of analysis of horizontal distance (D1–D5), vertical length (H0–H4), mesio–distal distance (W1–W3) and vertical height (PH1–PH3)

Weeks	D1	D2	D3	D4	D5
E16–20	16.4 ± 1.14	14.41 ± 1.09	5.57 ± 1.24	6.75 ± 0.95	2.31 ± 1.28
E21–25	20.04 ± 1.71***	18.28 ± 1.47***	9.78 ± 2.37***	10.0 ± 2.00***	5.01 ± 2.07***
E26–31	23.4 ± 1.27***	23.31 ± 2.57***	14.63 ± 1.71***	13.6 ± 1.45***	9.03 ± 1.74***
Weeks	H0	H1	H2	H3	H4
E16–20	10.3 ± 1.23	3.06 ± 0.34	2.12 ± 0.48	4.00 ± 0.69	1.66 ± 0.81
E21–25	12.36 ± 0.85**	3.8 ± 0.76*	3.58 ± 0.91***	6.36 ± 0.72***	3.04 ± 1.26***
E26–31	14.28 ± 1.67***	4.46 ± 0.38***	5.16 ± 0.47***	7.80 ± 0.38***	4.97 ± 0.87***
Weeks	W1	W2	W3	PH1	PH2	PH3
E16–20	2.78 ± 0.54	1.71 ± 0.49	2.04 ± 0.69	1.95 ± 0.25	3.82 ± 0.55	6.45 ± 1.04
E21–25	2.39 ± 0.42	1.65 ± 0.52	1.75 ± 0.69	1.87 ± 0.57	4.80 ± 0.70***	7.61 ± 0.62***
E26–31	2.34 ± 0.57	1.50 ± 0.19	1.65 ± 0.67	1.9 ± 0.78	5.22 ± 0.71***	7.94 ± 0.77***

E15–20 ($N = 10$, male = 9, female = 1, 20 sides), E21–25 ($N = 9$, male = 6, female = 3, 18 sides), E26–31 ($N = 6$, male = 3, female = 3,12 sides)

One-way ANOVA followed by Bonferroni's post-hoc comparisons tests were performed in all statistical analyses between E16–20 v.s. E21–25 or E16-–20 v.s. E21–25

*$p < 0.05$, **$p < 0.01$, ***$p < 0.001$

were only found in the PH2 and PH3 of E21–E25 and E26–E31 ($p < 0.001$).

Histological observations (Fig. 5)

At the E25, frontal sections revealed the developed nasal turbinates, including ST, MT and IT as onion-like structures along the lateral masses of the ethmoid in the NC. The woven bone structure was clearly discernible in the maxilla, V, cribriform of ethmoid bone, IT, MT and sphenoid bone. In contrast, immature ossification was found in the ST. A weak ossification zone appeared at the end of the anterior region of MT and IT in horizontal sections. In the sagittal section, the thin and elongated ossification zone of the ST was observed. This was similar to the calcified stick structure of the CBCT image of E25. In the frontal sections, the V appeared as a Y-like structure, located at the border of maxilla. This was similar to the Y-like structure of the CBCT image of E25. It was near the body of the sphenoid bone of sagittal section. The IT also appeared as an elongated structure compared to that of CBCT image.

Discussion

The IT is related to the narrowest part of the NC for nasal airway obstruction formation undergoing skeletal enlargement of the IT. Uzun et al. [26] showed that a lamellar structure of the IT had the highest frequency (352, 62.19%) in 566 specimens, and the morphological structure and volume of the IT is important during clinical evaluation. Three turbinate positions and relationships give useful information along with important anatomic landmarks for non-invasive endoscopic skull base and ear, nose and throat surgical procedures. Lee et al. [13] suggested that the structure of the anterior inferior part of the MT was useful for designing surgical treatment for partial MT, in contrast to other investigators for whom it was more important than the MT in terms of flow during inspiration. Our data showed these turbinate positions and relationships during the formation of ossification levels. Anatomic variations, including deviated nasal septum, IT hypertrophy, paradoxic MT and concha bullosa, are all associated with surgical correctable nasal obstructions [19]. Investigators reported that in human three turbinates (IT, MT, ST) with air space zones are clearly formed in the NC in early embryonic stages [3, 19, 27]. First, the embryonic ossification process of woven bone of the maxilla can be identified from E9 to E10 weeks and enlarge both absolutely and relatively to the NC [1]. At the E17 or E18 week, the ossification of the nasal capsule begins as well in the lateral half of the IT. The MT begins to ossify, extending at its free end. Subsequently, the ethmoido-turbinal structure appears between the 8th and 10th weeks of gestation [19]. In our results using CBCT, the IT and MT were found to be thin rod structures composed of a few small ossification masses at E16. The ossified ST appeared as a small mass at E21. The ossification stage of IT is similar to that of other reports [1, 3, 5]; however, the ST was calcified in structure late at E21 during development. From the E25 human foetus, clear ossification of the ST was found in the NC. In particular, the MT was developed from E25. MT and IT are important keys for successful endoscopic surgical treatment.

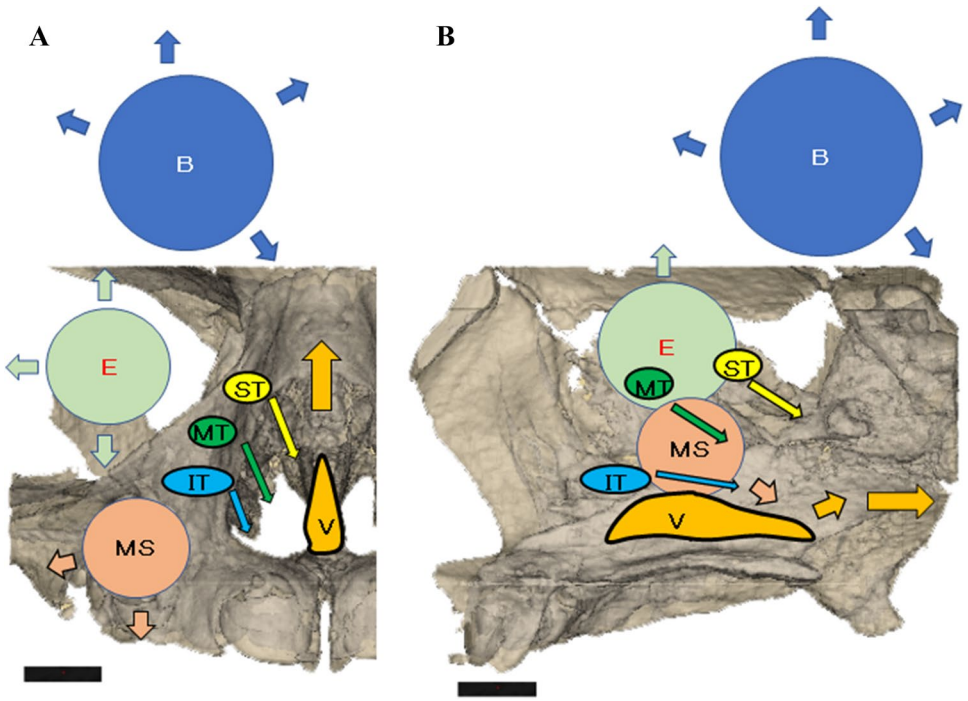

Fig. 6 The schematic images of growth direction of the NC and surrounding structures. Figure 6a, frontal view of schematic image of the NC; Fig. 6b, sagittal view of schematic image of the NC. The development of nasal turbinates with three elements: brain, eyeball, and maxillary sinus were shown. *B* brain, *E* eyeball, *IT* inferior turbinate, *MS* maxillary sinus, *MT* middle turbinate, *ST* superior turbinate, *V* vomer, Bar = 5 mm. (Color figure online)

At the formation of middle and inferior nasal concha, various nasal elements were already ossified and formed in the NC. The middle nasal concha was formed from the second ethmoturbinal material, the ST was formed from the third ethmoturbinal material and the ST was formed from the fourth ethmoturbinal material [22, 23]. These embryonic-specific features affect the formation of the MT and ST. Uzun et al. [26] also showed that the IT was one of the most important in terms of clinical evaluation. The morphological imbalance of the NCs is associated with nasal septal deviation, considered a common aetiology of nasal airway obstruction [12]. The morphological imbalance of the NCs may be related to NC formation during development. From E23 to E25 weeks, the Y-like structure is clearly developed, where the ST appears as a wide rhomboid-shaped structure. The V was located near the palatal bone horizontal plate and sphenoid bone. Our results indicated that the V was elongated and widely developed in the posterior–superior directions during NC development. The IT, MT and ST were also elongated in the posterior sagittal direction. In the frontal direction, the V was also elongated in the superior direction. The IT and MT developed in the inferior direction during the development of NC. In our measurement analyses, significant differences of measurement data of horizontal distances and vertical lengths of NC elements for nasal turbinates were found to be comparable to those of the mesio–distal distances. During development of the nasal turbinates, horizontal and vertical directions indicated a key to formation of the human NC in our statistical analysis.

The developed ST, MT, and IT are derived from the olfactory fascial units. In a new theory of formation of NC, this is separated from the brain by the cartilaginous olfactory capsule according to the evo–devo theory [7, 8]. Botti et al. [4] indicated the Vs were also derived from the secondary palate, along with the palatine processes of the maxilla. The palatine processes of the maxillae with the precursors of V bones are derived from midline fusion, posterior to the primary palate. The nasal septum and the perpendicular plate of the ethmoid are related to the formation of maxilla during development. The origin of the ethmoid sinus is different from the other sinus according to the evo–devo theory [9]. Therefore, the evo–devo theory states that the origin of each nasal element may be derived from extension or elongated of nasal turbinates during development. Our results showed that the ossification levels of the ethmoid bone, IT, and maxilla were different at each developmental stage, which was related to the formation of the NC. Specifically, the ossification of the nasal capsule begins in the lateral half of the IT at E17–E18 [1, 3] in comparison to that of MT at E20–E22. The different ossification levels between IT and MT was also related to the three development movements such as the frontalization of eye, development of frontal lobe, and regression of midface [15, 17]. Based on these results, we hypothesize the following: We also offered three hypotheses: (1) development of the brain, eye sockets and orbits, paranasal sinuses, particularly the MS (Fig. 6). The location of the MT and ST were later moved to the posterior of the NC in contrast to the IT and V which movement may be related to different origin by the evo–devo theory. During

the E17 week of development, the invagination of the mucus layer invaded the maxillary bone, constituting the MS. At the E36 week, the lateral nasal wall is well developed. In 23 foetuses, the ST was found [18]. Pneumatization of the paranasal sinuses gradually occurs between the ages of 4 and 8 years and accelerates between the ages of 8 and 12 years [27]. Our results suggested the elongated direction of the IT and MT towards the sphenoidal bone. Therefore, the movement of location in the ST, MT and IT are important keys during formation of the NC in human embryonic stages. Especially for the MT, development is the most important element of the structure of NC.

Conclusions

More detailed morphological information of nasal turbinates is needed for endoscopic surgical treatment. We investigated the morphological data of NC and nasal turbinates in human foetuses using CBCT and macroscopic observations in detail. The MT elongated development is most important for NC formation in the ossification levels of the elements of the nose. The measurement data of the NC indicated that horizontal and vertical directions of nasal turbinates affect the formation of the human NC. This information may provide useful data for nasal sinus and nasal turbinate formation of nose in the field of otolaryngology and childhood clinical treatments.

Author contributions Protocol/project development IS, RA. Data collection and management RA, TK. Data analysis YM. Manuscript writing/editing RA, TK, IS.

Compliance with ethical standards

Conflict of interest The authors declare that they have no conflicts of interest.

References

1. Arredondo de Arreola G, López Serna N, de Hoyos Parra R, Arreola Salinas MA (1996) Morphogenesis of the lateral nasal wall from 6 to 36 weeks. Otolaryngol Head Neck Surg 114:54–60
2. Arslan H, Aydinlioğlu A, Bozkurt M, Egeli E (1999) Anatomic variations of the paranasal sinuses: CT examination for endoscopic sinus surgery. Auris Nasus Larynx 26:39–48
3. Bingham B, Wang RG, Hawke M, Kwok P (1991) The embryonic development of the lateral nasal wall from 8 to 24 weeks. Laryngoscope 101:992–997
4. Botti S, Rumeau C, Gallet P, Jankowski R (2017) Vomero-premaxillary joint: a marker of evolution of the species. Eur Ann Otorhinolaryngol Head Neck Dis 134(2):83–87. https://doi.org/10.1016/j.anorl.2016.11.002. (**Epub 2017 Jan 20**)
5. Cankaya H, Egeli E, Kutluhan A, Kiriş M (2001) Pneumatization of the concha inferior as a cause of nasal obstruction. Rhinology 39:109–111
6. Herzallah IR, Saati FA, Marglani OA, Simsim RF (2016) Retromaxillary pneumatization of posterior ethmoid air cells: novel description and surgical implications. Otolaryngol Head Neck Surg 155:340–346. https://doi.org/10.1177/0194599816639943. (**Epub 2016**)
7. Jankowski R (2013) The evo-devo origin of the nose, anterior skull base and midface. Springer, Paris
8. Jankowski R, Rumeau C, de Saint Hilaire T, Tonnelet R, Nguyen DT, Gallet P, Perez M (2016) The olfactory fascia: an evo-devo concept of the fibrocartilaginous nose. Surg Radiol Anat 38(10):1161–1168. (**Epub 2016**)
9. Jankowski R, Márquez S (2016) Embryology of the nose: the evo-devo concept. World J Otorhinolaryngol 6(2): 33–40. https://doi.org/10.5319/wjo.v6.i2.33
10. Jankowski R, Perrot C, Nguyen DT, Rumeau C (2016) Structure of the lateral mass of the ethmoid by curved stacking of endoturbinal elements. Eur Ann Otorhinolaryngol Head Neck Dis 133(5):325–329. https://doi.org/10.1016/j.anorl.2016.07.007. (**Epub 2016**)
11. Kantarci M, Karasen RM, Alper F, Onbas O, Okur A, Karaman A (2004) Remarkable anatomic variations in paranasal sinus region and their clinical importance. Eur J Radiol 50:296–302
12. Kim SK, Heo GE2, Seo A, Na Y, Chung SK (2014) Correlation between nasal airflow characteristics and clinical relevance of nasal septal deviation to nasal airway obstruction. Respir Physiol Neurobiol 192:95–101. https://doi.org/10.1016/j.resp.2013.12.010. (**Epub 2013**)
13. Lee KB, Jeon YS, Chung SK, Kim SK (2016) Effects of partial middle turbinectomy with varying resection volume and location on nasal functions and airflow characteristics by CFD. Comput Biol Med 77:214–221. https://doi.org/10.1016/j.compbiomed.2016.08.014. (**Epub 2016**)
14. Liu ZP, Luo JW, Xu GZ, Gao L, Yi JL, Huang XD, Qu Y, Wang K, Zhang SP, Xiao JP (2017) Failure patterns and prognostic factors of patients with primary mucosal melanoma of the nasal cavity and paranasal sinuses. Acta Otolaryngol 137:1115–1120. https://doi.org/10.1080/00016489.2017.1336797. (**Epub 2017**)
15. Márquez S, Tessema B, Clement PA, Schaefer SD (2008) Development of the ethmoid sinus and extramural migration: the anatomical basis of this paranasal sinus. Anat Rec (Hoboken) 291(11):1535–1553. https://doi.org/10.1002/ar.20775
16. Marquez S, Pagano A, Lawson W, Laitman J (2016) Evolution of the human nasal respiratory tract: nose and paranasal sinuses. Sataloff's comprehensive textbook of otolaryngology: head and neck surgery (Rhinology/Allergy and Immunology), 2, JP Medical Ltd., New Delhi, 17–42
17. Moore W (2009) The mammalian skull. Biological structure and function. Cambridge University Press, Cambridge
18. Nakashima T, Kimmelman CP, Snow JB Jr (1984) Structure of human fetal and adult olfactory neuroepithelium. Arch Otolaryngol 110(10):641–646
19. Neskey D, Eloy JA, Casiano RR (2009) Nasal, septal, and turbinate anatomy and embryology. Otolaryngol Clin North Am 42(2):193–205. https://doi.org/10.1016/j.otc.2009.01.008.
20. Schepelmann K (1990) Erythropoietic bone marrow in the pigeon: development of its distribution and volume during growth and pneumatization of bones. J Morphol 203(1):21–34
21. Selcuk A, Ozcan KM, Ozcan I, Dere H (2008) Bifid inferior turbinate: a case report. J Laryngol Otol 122:647–649. (**Epub 2007**)
22. Som PM, Naidich TP (2013) Illustrated review of the embryology and development of the facial region, part 1: early face and lateral nasal cavities. Am J Neuroradiol 34:2233–2240. https://doi.org/10.3174/ajnr. (**A3415. Epub 2013**)
23. Som PM, Naidich TP (2014) Illustrated review of the embryology and development of the facial region, part 2: late development of the fetal face and changes in the face from the newborn to

adulthood. Am J Neuroradiol 35:10–18. https://doi.org/10.3174/ajnr.A3414. (**Epub 2013**)
24. Stenner M, Rudack C (2014) Diseases of the nose and paranasal sinuses in child. GMS Curr Top Otorhinolaryngol Head Neck Surg 13:Doc10. https://doi.org/10.3205/cto000113. (**eCollection 2014**)
25. Streeter GL (1951) Developmental horizons in human embryos. Age groups XI to XXIII Embryol Reprint Vol II Carnegie Inst, Washington
26. Uzun L, Ugur MB, Savranlar A, Mahmutyazicioglu K, Ozdemir H, Beder LB (2004) Classification of the inferior turbinate bones: a computed tomography study. Eur J Radiol 51:241–245
27. Wolf G, Anderhuber W, Kuhn F (1993) Development of the paranasal sinuses in children: implications for paranasal sinus surgery. Ann Otol Rhinol Laryngol 102:705–711